Damping contributions of coatings to the viscoelastic behaviour of mechanical components

Stefano Amadori , Giuseppe Catania

Department of Industrial Engineering – Ciri MaM, University of Bologna
Viale Risorgimento 2, 40136 Bologna, Italy
stefano.amadori4@unibo.it, giuseppe.catania@unibo.it

Abstract

Coating layer technology is known in literature as an effective tool for modifying the viscoelastic behaviour of materials. In this work various coating solutions are investigated in order to estimate their contribution to the dissipative behaviour of mechanical components. Different production processes are used to apply single-layer and dual-layer coatings of Al oxide, Ti and TiO_2 , Cr and CrN to uncoated specimens made of Al, stainless steel and harmonic steel. Force and displacement experimental data obtained from forced excitation dynamic mechanical measurements are used to find the specimen constitutive equation estimated parameters. A high order generalized Kelvin model is adopted to model the constitutive equivalent material relationship of coated specimens in the form of the ratio of two polynomials expressed as a function of frequency. The model parameters are numerically identified and the model reduced and optimized by means of a robust identification technique.

1 Introduction

Composites obtained from coating deposition techniques are non-conventional materials designed to have specialized mechanical properties. The study of their dynamic behaviour can be of great interest for industrial, aerospace and automotive mechanical applications where high stiffness and high resistance components are commonly employed. In modern high speed applications unwanted vibrations may result due to the inertial forces. Vibrations may cause an excessive noise level, a decrease in the system efficiency and a shortening of the system service life. By increasing the component dissipative properties, high vibration levels may be damped. The use of coating layers may help in achieving this result while at the same time maintaining the components original high stiffness and resistance [1-3].

Coating layer technology includes many different deposition techniques, for example plasma spray, the anodization process or plasma vapour deposition [4,5]. Layer composition, single or multi layered structure, and adhesion to the substrate are all factors that must be taken into account when studying the properties of coatings and many researchers investigated the influence of the coating characteristics, such as the coating material structure [6-8] or the interface structure [9] on the coated component damping behaviour at various temperatures [10]. The deposition of layers with high internal hysteresis or with high frictional actions between the different layers can be an effective solution to significantly increase the dissipative properties of a component [6,11,12].

The use of dynamic mechanical measurements, in both forced or free vibration condition, is a well-known method to investigate the damping behaviour of a wide range of materials and specimen geometric parameters and was also employed [13-15] to estimate the improved damping behaviour in coated components by means of direct comparison with uncoated ones.

The constitutive relationship for coated components may not be accurately described by known models [16,17] because single or multi-layered coated materials dynamic behaviour can be considerably complex [18]. This can lead to the adoption of high order constitutive models [19-21] that may require the use of not trivial constitutive equations. The problem of identifying such constitutive equation parameters is generally ill-conditioned and a robust identification procedure must be considered in order to solve it [18,22].

In this work different coating solution applied on a metal substrate by means of different techniques are investigated. The dynamic mechanical measurement are processed by means of a robust parameter

identification and model condensation technique and the processed measurements data results, related to coated and uncoated specimens, are compared.

2 Identification procedure

The identification procedure used to identify the specimen constitutive equivalent material relationship in the frequency domain was defined by the authors of this work in a previous paper [18]. Here it is briefly outlined how force and displacement experimental tests data are processed.

2.1 Constitutive relationship experimentally estimated value

The frequency dependent constitutive relationship between the Fourier transform of stress ($\hat{\sigma}$) and strain ($\hat{\varepsilon}$) can be expressed as:

$$\hat{\sigma} = E(\omega) \cdot \hat{\varepsilon} \tag{1}$$

Dynamic mechanical measurements can be used to obtain the value of $E(\omega)$ in the desired frequency range. In this work only specimens in the form of slender beams in a single-cantilever experimental set-up with clamped-sliding boundary conditions and excited by means of a periodic force applied at the beam sliding end are considered. Taking into account the contribution of inertial forces, the relationship between the applied periodic force $Q(t) = Q_0 \exp(j\omega t)$ and the transverse displacement $v(t)$ at the sliding end of the beam in the frequency domain can be approximated by Eq.2.

$$\hat{v}(\omega) \simeq \sum_{i=1}^{N} \frac{\left[2\left(1-\cosh k_i \cdot \cos k_i\right)/\left(\sinh k_i + \sin k_i\right)\right]^2}{-M \cdot \omega^2 + E(\omega) \cdot k_i^4 \cdot I/L^3} \cdot \hat{Q}(\omega) \tag{2}$$

$\hat{v}$ and $\hat{Q}$ are the Fourier transform of transverse displacement and applied force respectively, M is the beam mass, L is the beam length and I the beam section moment. k_i are values satisfying the condition $\sinh k \cos k + \cosh k \sin k = 0$. Eq.2 can be used together with the corresponding force and displacement data at frequencies ω_r to define the equation:

$$X\left(E(\omega_r)\right) = \sum_{i=1}^{N} \frac{\left[2\left(1-\cosh k_i \cdot \cos k_i\right)/\sinh k_i + \sin k_i\right]^2}{-M \cdot \omega_r^2 + E(\omega_r) \cdot k_i^4 \cdot I/L^3} - \frac{\hat{v}(\omega_r)}{\hat{Q}(\omega_r)} = 0 \tag{3}$$

The Newton Raphson method is used to find the solutions of Eq.3, that are the experimentally estimated values of $E(\omega)$ at frequencies ω_r .

2.2 Constitutive model identification

The constitutive equivalent material relationship is modelled by means of a generalized Kelvin model of order *n*, i.e. made up of a series of *n* single Kelvin unit, and Eq.1 becomes:

$$\hat{\sigma} = E_0 \cdot D(\omega) \cdot \hat{\varepsilon} \tag{4}$$

with:

$$E_0 = \left(\sum_{i=1}^{n} \frac{1}{E_i} \right)^{-1} \quad , \quad D(\omega) = \frac{1 + \sum_{r=1}^{n} \left(a_r \cdot \omega^r \right)}{1 + \sum_{s=1}^{n-1} \left(b_s \cdot \omega^s \right)} . \tag{5}$$

E_0 is a constant and represent the modulus of the material at zero frequency. It can be extrapolated from dynamical measurement test results as the frequency approach zero, or alternatively from static experiments, i.e. creep and stress relaxation tests. *D(ω)* express the frequency dependence of the modulus in the form of the ratio of two polynomials with unknown coefficients a_r and b_s.

The coefficients of the two polynomials can be obtained by means of an approach based on the least square error technique and of the experimentally estimated values of $D(\omega_r)$ at frequencies ω_r [18]. *D(ω)* is first expressed by means of an orthogonal polynomial basis made up of Forsythe orthogonal polynomials $c_s(\omega)$ and $d_r(\omega)$:

$$D(\omega) = \frac{1 + \sum_{s=1}^{n} \alpha_s \cdot c_s(\omega_i)}{1 + \sum_{r=1}^{n-1} \beta_r \cdot d_r(\omega_i)} \tag{6}$$

The least square error technique is then used to obtain coefficients α_s and β_r [22]. The Forsythe orthogonal polynomial basis [23] is adopted in order to assure a high accuracy for the identification of both low and high order models because high order model coefficient calculations can be affected by ill-conditioning. A known algorithm [24] is used to convert back the polynomials coefficients to coefficients in an equivalent monomial base, obtaining an expression of *D(ω)* equivalent to that of Eq.3. This conversion is made in order to obtain the constitutive equivalent material relationship in a more convenient form suitable to further processing and manipulation.

2.3 Condensation of the constitutive model

The constitutive model obtained from the previous subsection procedure is generally of a high order. This is also a consequence of the fact that experimental measurements are affected by noise while the basic least square error technique cannot differentiate between physical system poles and virtual noise generated non-physical ones. It can be useful to condense the identified model by eliminating its non-physical components. An optimised model of significantly lower order but with accuracy comparable to non-condensed models of significantly higher order, can be obtained.

Eq.4 can be rewritten in the standard partial fraction form where poles g_i and residues R_i of the rational function *1/D(ω)* are outlined:

$$\hat{\varepsilon}(\omega) = \frac{1}{E_0} \cdot \sum_{i=1}^{n} \frac{R_i}{(j\omega - g_i)} \cdot \hat{\sigma}(\omega) \tag{7}$$

Poles and residues are expected to be found as complex conjugated pairs or real values, and in both cases with a negative real part. Physical poles are also expected to show stability as the model order is increased. Poles with positive real part or varying with respect to model order *n* can be regarded as non-physical and discarded from the condensed model. The final expression of the constitutive equivalent material model, described by a subset of *m* physical pole-residue couples Rc_i and gc_i from $\{R_i, g_i\}$ is given by:

$$\frac{1}{D(\omega)} \simeq \sum_{i=1}^{m} \frac{Rc_i}{(j\omega - gc_i)} + S_h(\omega) \quad ; \quad S_h(\omega) = \sum_{k=0}^{h} l_k \cdot (j\omega)^k \tag{8}$$

The contribution of the discarded pole-residue pairs is accounted by means of the polynomial function $S_h(\omega)$, and coefficients l_k can be obtained by a calculation procedure found in these authors previous work [18].

3 Experimental measurements: results and discussion

Tested specimens are in the form of slender beam of rectangular cross section with length 10^{-2}m, width 3×10^{-3}m, thickness 5×10^{-4}m. The coatings are applied on opposite faces of the beam.

Three different coating solutions applied on different metallic substrates are considered in this work. The first solution consists of single layer coatings of Al oxide, 40μm thickness, applied on an Al1000 substrate by means of an anodizing process. The other two solutions are obtained with the reactive plasma deposition (RPVD) technique. Two different type of dual-layer coatings, both formed by a metallic bond coat (1μm thickness) covered by an harder coating layer (1μm thickness), are deposited on different metallic substrates, i.e. C67 steel, AISI 304 stainless steel and Al1000 Al alloy. The first solution adopts Ti an TiO_2 for the metallic bond coat and the harder oxide layer respectively, while in the second solution Cr is used for the bond coat layer and a CrN for the nitride hard layer.

The specimens are tested with forced flexural excitation in a single-cantilever (clamped-sliding boundary conditions) experimental set-up. Dynamic measurements at 0.01% maximum strain over a [0.01-200]Hz frequency range and 35°C constant temperature are made on coated and uncoated specimen sets with a Dynamic Mechanical Analyzer (DMA). Applied force and transverse displacement data are obtained and processed with the procedure presented in section 2.

3.1 Results

Figs.1-7 show, for the different coating solution and substrate combinations, the experimentally estimated values of the ratio *Im(D)/Re(D)* of the imaginary and real part of *D(ω)*, taken as a measure of the specimen damping behaviour, and the relative difference of such ratio with respect to the values obtained from uncoated specimen tests. It can be observed that C67 steel and AISI 304 stainless steel specimens with the Ti+TiO_2 dual-layer coating show the same damping behaviour of uncoated specimens (Figs.1,6).

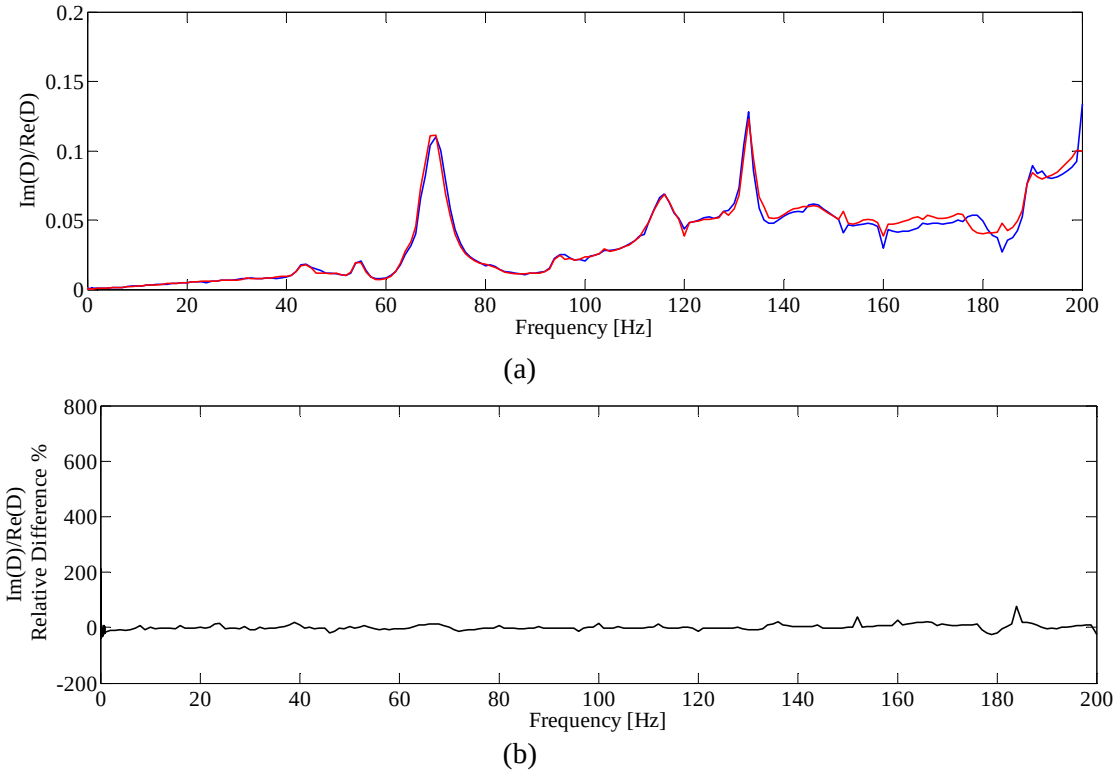

Figure 1: (a) Estimated values of *Im(D(ω))/Re(D(ω))* ratio for dual-layer Ti+TiO_2 coated C67 steel specimen (red) and homogeneous C67 steel specimen (blue), and (b) *Im(D(ω))/Re(D(ω))* relative difference.

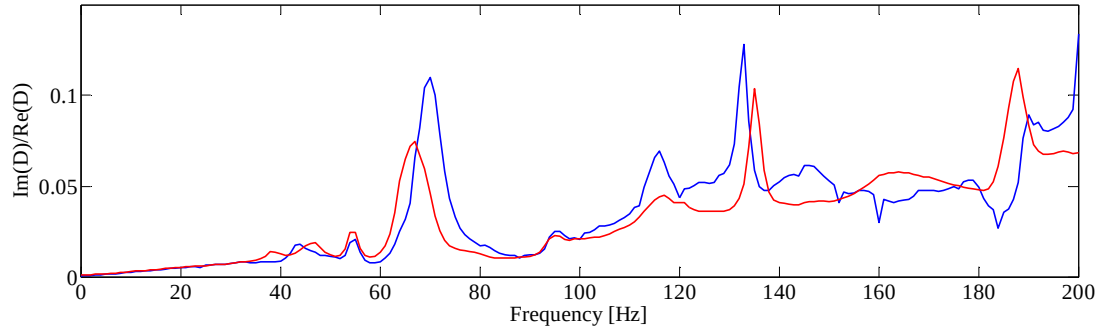

(a)

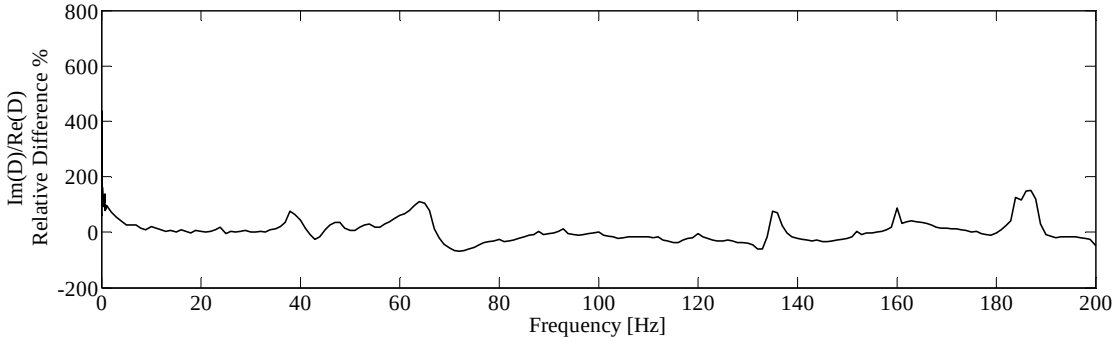

(b)

Figure 2: (a) Estimated values of *Im(D(ω))/Re(D(ω))* ratio for dual-layer Cr+CrN coated C67 steel specimen (red) and homogeneous C67 steel specimen (blue), And (b) *Im(D(ω))/Re(D(ω))* relative difference.

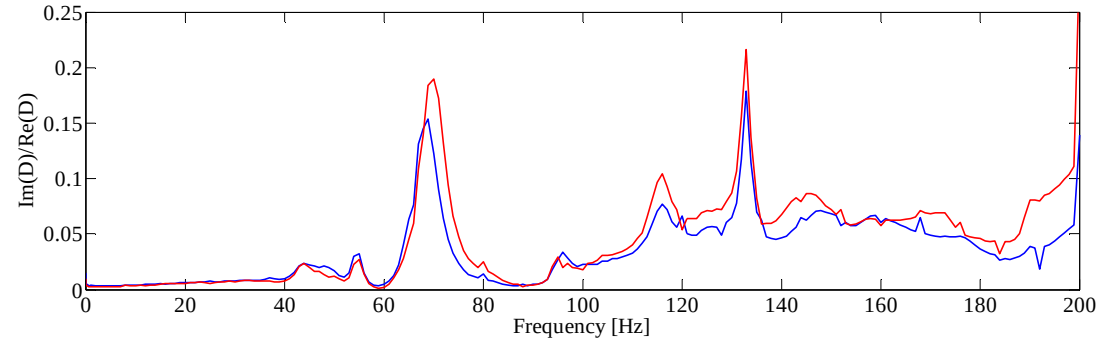

(a)

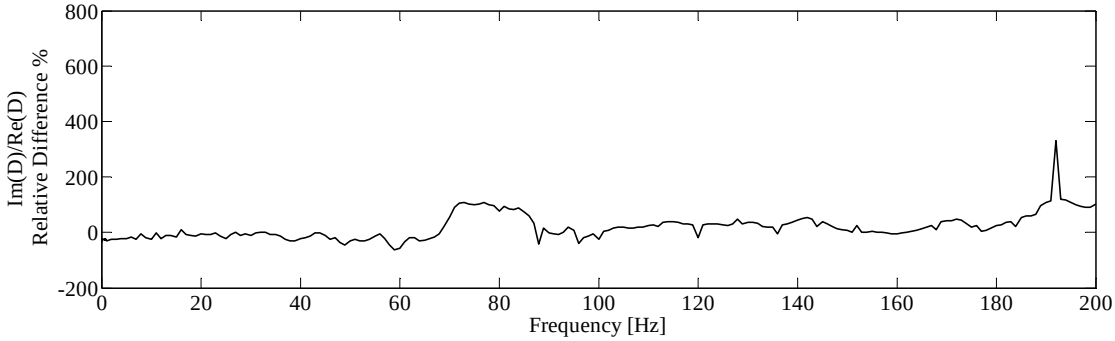

(b)

Figure 3: (a) Estimated values of *Im(D(ω))/Re(D(ω))* ratio for dual-layer Ti+TiO_2 coated Al1000 specimen (red) and homogeneous Al1000 specimen (blue), and (b) *Im(D(ω))/Re(D(ω))* relative difference.

For beams coated with the Cr+CrN dual-layer coating solution, specimens with the three different substrates, i.e. C67 - Aisi304 steel and the Al1000 alloy, present a similar damping behaviour (Figs.2,4,7), since the ratios *Im(D)/Re(D)* of coated and uncoated specimens only present slight differences over the tested frequency range. Of particular interest are the damping behaviours shown by the Al1000 specimens coated with the Ti+TiO_2 dual-layer and with the Al oxide single-layer (Figs.3,5). In both cases the *Im(D)/Re(D)* ratio is higher for the coated specimens than for the uncoated ones. The condensed constitutive equivalent material models for these two specimens are reported in Figs.8-9 and compared with the experimentally estimated values and a computational non-condensed model.

3.2 Discussion

Observing the presented results only two (Figs.3,5) of the seven different coated specimen typologies show an improved damping behaviour with respect to uncoated specimens. In both cases the substrate material is the Al1000 alloy . It can be noted that the Ti+TiO_2 dual coating applied on harmonic steel and stainless steel seems to have no effects on the specimen dissipative properties (Figs.1,6). The dual-layer coating thickness, structure and composition is the same for all three substrate materials, and this result indicates that the damping behaviour improvement might be due to the energy dissipated by the friction actions at the interface between the Ti bond coat layer and the Al alloy. Such a difference is not observed for Cr+CrN coating layers, whose effect does not appear significant over the tested frequency range and it is not related to the type of substrate employed (Figs.2,4,7).

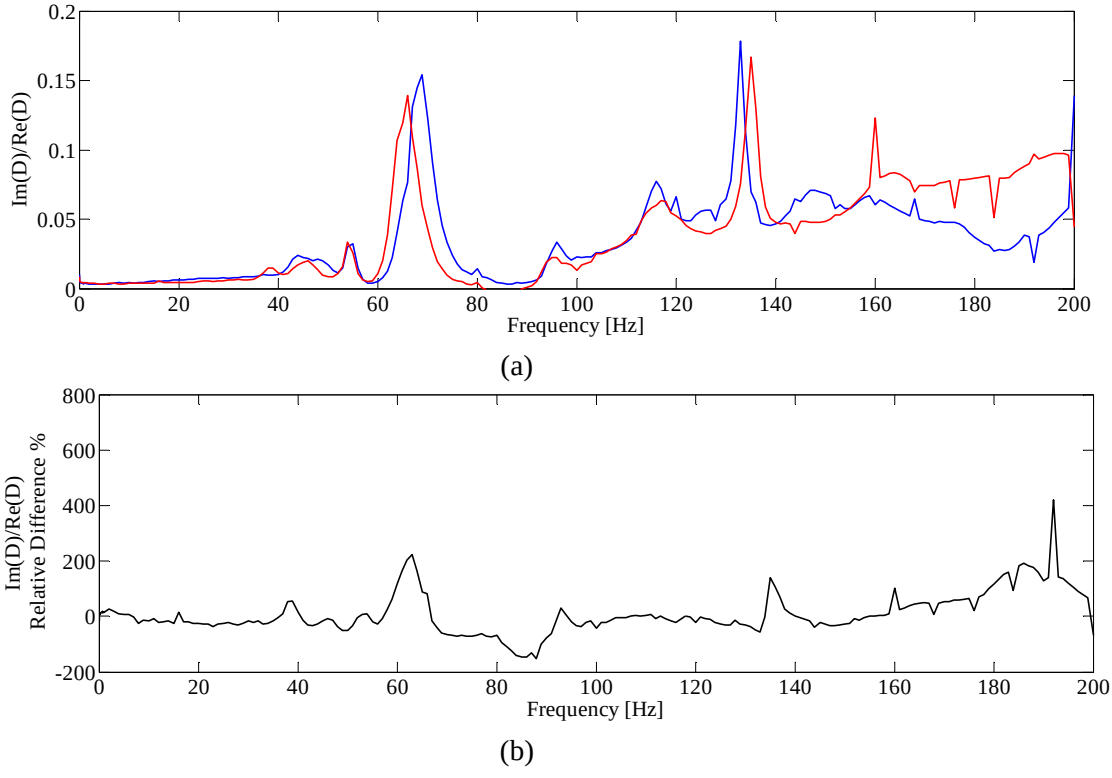

Figure 4: (a) Estimated values of *Im(D(ω))/Re(D(ω))* ratio for dual-layer Cr+CrN coated Al1000 specimen (red) and homogeneous Al1000 specimen (blue), and (b) *Im(D(ω))/Re(D(ω))* relative difference.

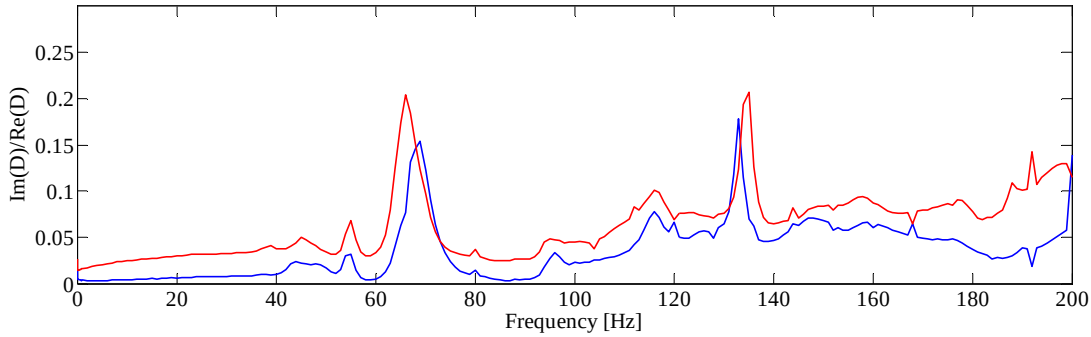

(a)

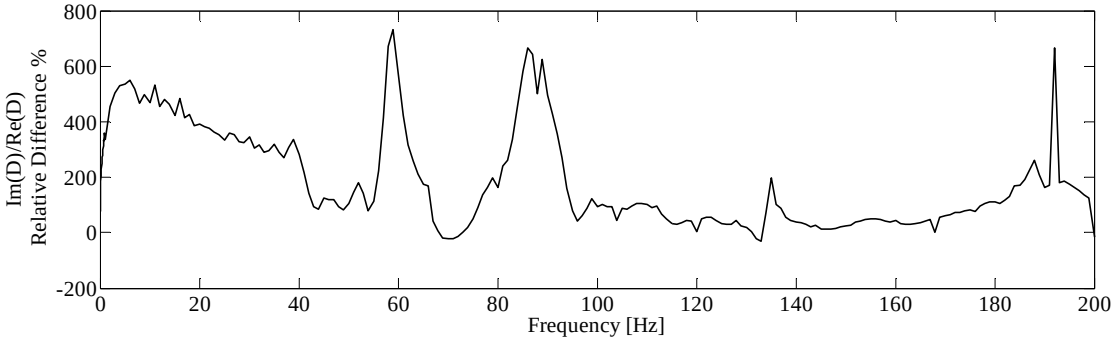

(b)

Figure 5: (a) Estimated values of *Im(D(ω))/Re(D(ω))* ratio for single-layer Al-oxide coated Al1000 specimen (red) and homogeneous Al1000 specimen (blue), and (b) *Im(D(ω))/Re(D(ω))* relative difference.

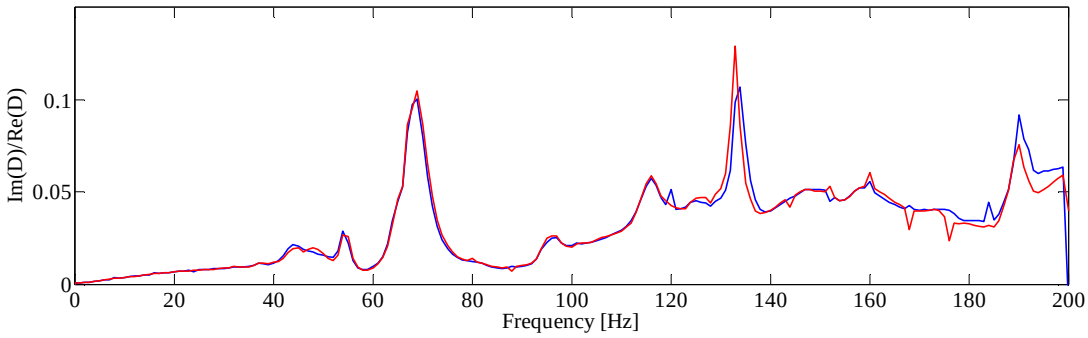

(a)

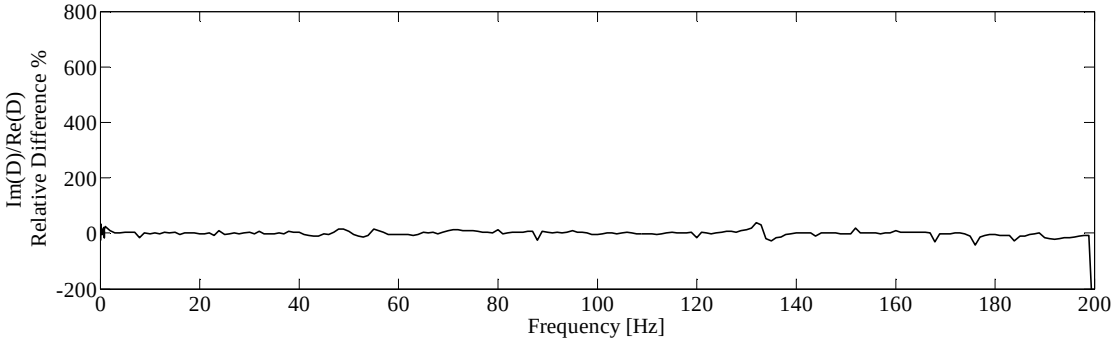

(b)

Figure 6: (a) Estimated values of *Im(D(ω))/Re(D(ω))* ratio for dual-layer Ti+TiO_2 coated AISI 304 specimen (red) and homogeneous AISI 304 specimen (blue), and (b) *Im(D(ω))/Re(D(ω))* relative difference.

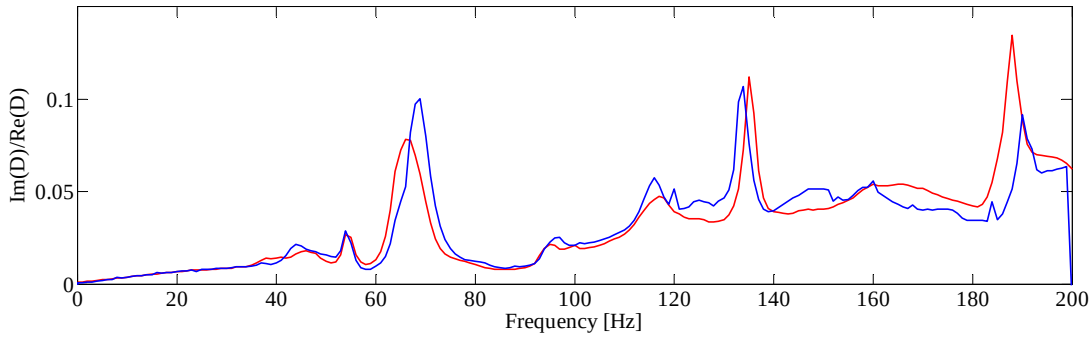

(a)

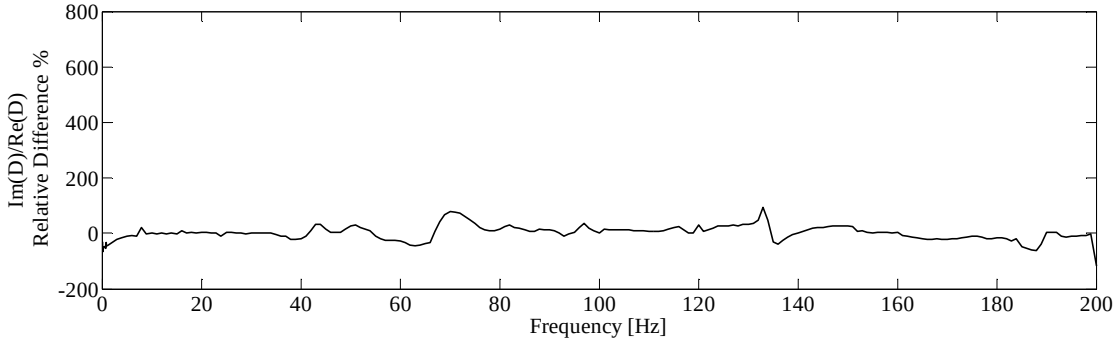

(b)

Figure 7: (a) Estimated values of *Im(D(ω))/Re(D(ω))* ratio for dual-layer Cr+CrN coated AISI 304 specimen (red) and homogeneous AISI 304 specimen (blue), and (b) *Im(D(ω))/Re(D(ω))* relative difference.

Differences can be noted also for the Ti+TiO_2 and the Al oxide coating solutions applied on the same Al1000 substrate. Application of the single-layer Al oxide coating significantly increase the *Im(D)/Re(D)* ratio across all the measured frequency range and shows a notable and stable effect for frequencies below 50Hz. The effect of the dual-layer Ti+TiO_2 coating is noticeable only for frequencies above 70Hz. The difference in magnitude of the *Im(D)/Re(D)* with respect to the single-layer Al oxide and the dual-layer Ti+TiO_2 coatings can be due to the different thickness of the two coating layers. These two coating solutions can be considered a possible tool for the improvement of the damping behaviour of Al components. For both coating solutions a condensed model of relatively low order (n=13) was obtained and is shown in Figs.8-9. Such model is obtained by condensing a high order model (n=43).

It is desirable for a coated components to possess other characteristics than effective vibrational damping, i.e. the coating layer should modify the component geometry as little as possible, it should ensure a good statical and kinetical substrate adhesion, exhibiting a good fatigue strength after prolonged cyclic loading. This latter aspect in particular has to be verified by repeated cycle loading tests that are still to be completed at the time of this work.

Another aspect that deserve deeper analysis is the modelling of the coated beams. While the presented condensed model is useful in order to obtain the material constitutive relationship, it cannot be used to design different composite coating solutions than the one previously tested. For investigating and designing multi-layered specimens an effective model should be able to take into account the different characteristics of layers made of different materials, and also the interaction at the interface between layers. An extended multi-layer beam theory is being considered as a modelling tool with better predictive capabilities for the study of multi-layered specimens.

At the time of this work the multi-layer model is still at the development stage. Some preliminary key features of this multi-layer model are presented in the next section.

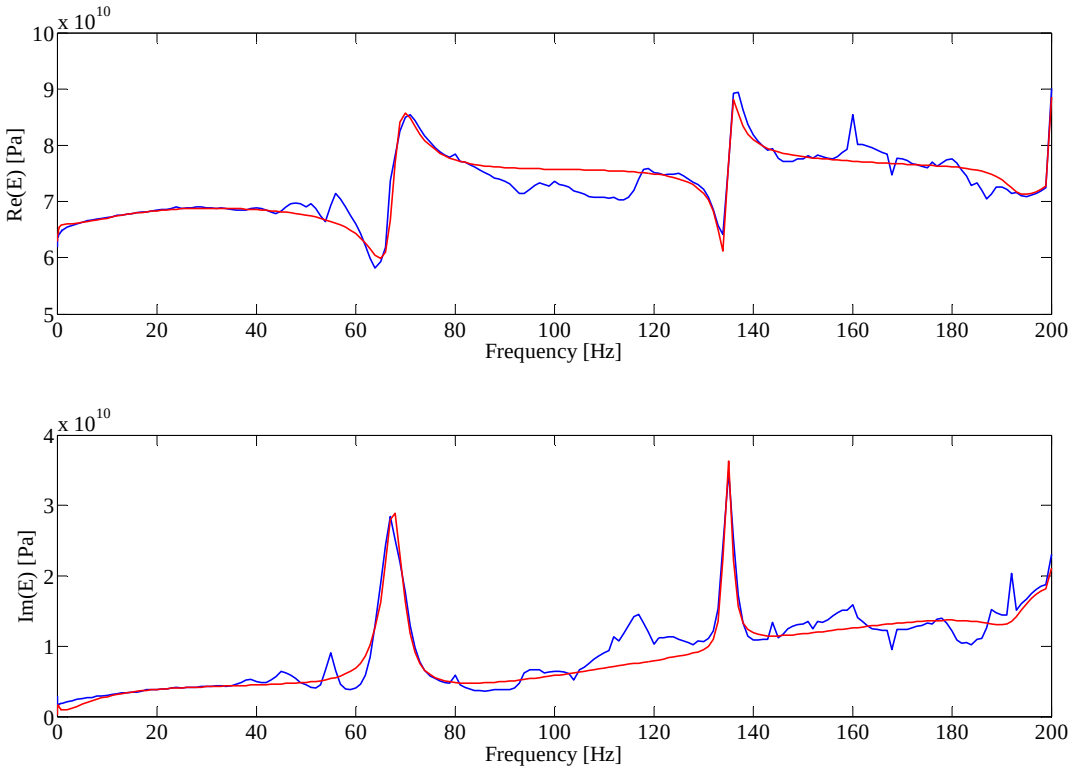

Figure 8 – Single-layer (Al oxide) coated Al1000 specimen:
E(ω) experimental estimates (blue), condensed model (*n*=13).

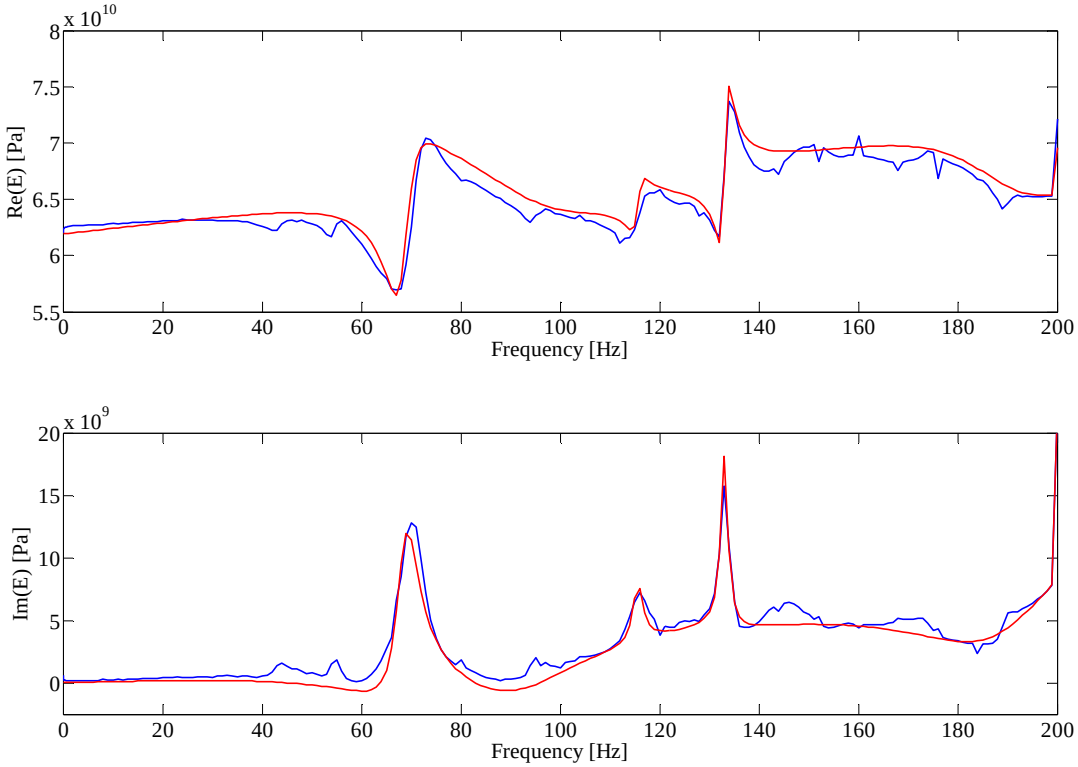

Figure 9 – Dual-layer ($Ti+TiO_2$) coated Al1000 specimen:
E(ω) experimental estimates (blue), condensed model (*n*=13) fitting estimate (red).

3.3 Multi-layer beam model

The classic Bernoulli-Euler and Timoshenko beam theories can be modified to deal with composite multi-layered beams, where the layers have significantly different parameter values. High-order beam theories, e.g. layer-wise theories [25-26], that takes into account the stress strain relationship of the single layers can be taken into account. Usually in layer-wise beam theories the number of kinematic variables employed increase with the number of layers and this can lead to high computational load if composites with a high number of layers are considered. In the so called zig-zag beam theories (a specific sub-type of layer-wise theory) the number of kinematic variables does not depend on the number of layers, and it is assumed that the longitudinal displacements present a pattern different from the Euler-Bernoulli linear standard pattern and that the transverse shear stress display continuity along the beam thickness and at the interface between the layers. The base for the multi-layer beam model being taken into account is a non-linear third-order theory of multi-layered shells [27].

In Fig.10 it is schematically represented the most simple case of multi-layered beam, a dual-layer beam, with rectangular cross section $A = H \cdot w$, and constituted by two layers of generally different thickness h_1 and $h_2=H-h_1$. Fig.11 shows a possible longitudinal displacements pattern related to the same dual-layer case example. It is assumed that for each layer the stress (σ), shear stress(τ), strain (ε), and shear strain(γ) relationships are:

$$\sigma_{xx} = E_i \cdot \varepsilon_{xx} \quad ; \quad \tau_{xy} = G_i \cdot \gamma_{xy} \quad ; \quad i = 1,2 \tag{9}$$

Where E_i and G_i are the axial (*xx* direction) and shear (*xy* direction) of the i-th layer. Strain and shear strain in terms of the longitudinal displacement *u(x,y,t)* and transverse displacement *v(x,t)* (that is considered not dependent from *y*) are defined by :

$$\varepsilon_{xx} = u' + \frac{(v')^2}{2} \quad ; \quad \gamma_{xy} = \frac{\partial u}{\partial y} + v' \tag{10}$$

$(\,)'$ represent the derivate with respect to the *x* coordinate. At the layer interface ($y=h_1$) the continuity of *u(x,y,t)* and τ_{xy}*(x,y,t)* is enforced:

$$u_{layer1}(x,h_1,t) = u_{layer2}(x,h_1,t) \quad ; \quad \tau_{layer1}(x,h_1,t) = \tau_{layer2}(x,h_1,t) \tag{11}$$

Longitudinal and transverse displacements that fulfils Eq.11 can be expressed in the form [25]:

$$v = v(x,t) \quad ; \quad u = u(x,y,t) = u_0(x,t) - y \cdot v'(x,t) + F(y)\phi(x,t) \tag{12}$$

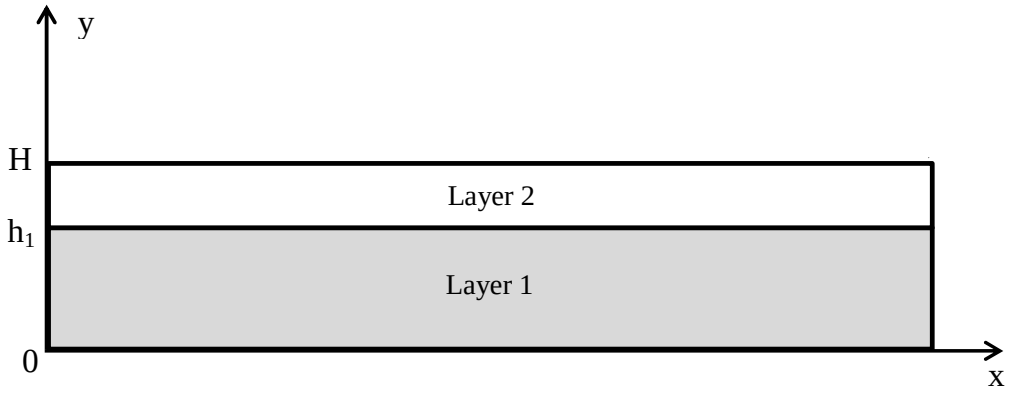

Figure 10 – Dual-layer beam schematic representation

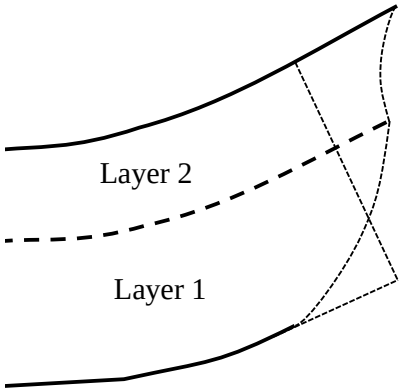

Figure 11 – Schematic representation of a third-order zig-zag model longitudinal displacement pattern for a dual-layer beam

v, u_0 and ϕ are the three displacement variables used to describe the beam motion and this is also true for beams with an arbitrary number of layers. $F(y)$ is piecewise cubic function of y and is dependent from E_i, G_i. and h_i (i=1,2).

The equations of motion as an explicit function of the three displacement variables can be obtained from the virtual work principle. It is considered a generic dual-layer beam with applied force Q directed along the y axis and perfectly bonded interfaces between layers:

$$\int_V (\sigma \cdot \delta\varepsilon)\, dV + \int_V (G \cdot \delta\gamma)\, dV = -\int_V (\rho \cdot \ddot{u} \cdot \delta u + \rho \cdot \ddot{v} \cdot \delta v)\, dV + \int_\Gamma (Q \cdot \delta v)\, d\Gamma \tag{14}$$

Where Γ is the beam section perpendicular to the y axis. The equations of motion results:

$$\begin{cases} K_1 \cdot u_0'' - K_2 \cdot v''' + K_3 \cdot \phi'' + K_1 \cdot v' \cdot v'' = M_1 \cdot \ddot{u}_0 - M_2 \cdot \ddot{v}' + M_3 \cdot \ddot{\phi} \\ K_2 \cdot u_0''' - K_4 \cdot v^{iv} + K_5 \cdot \phi''' + K_2 (v'' \cdot v'' + v' \cdot v''') + N \cdot v'' + N' \cdot v' + Q = M_2 \cdot \ddot{u}_0' - M_4 \cdot \ddot{v}'' + M_5 \cdot \ddot{\phi}' + M_1 \cdot \ddot{v} \\ K_3 \cdot u_0'' - K_5 \cdot v''' + K_6 \cdot \phi'' + K_3 \cdot v' \cdot v'' - K_7 \cdot \phi = M_3 \cdot \ddot{u}_0 - M_4 \cdot \ddot{v}' + M_6 \cdot \ddot{\phi} \end{cases} \tag{15}$$

The dependence from the different layer material stress-strain relationship is taken into account by means of K_i (i=1, … ,7), N and M_r (r=1, … ,6) defined by:

$$\begin{aligned} &K_1 = \int_0^{h_1} E_1 dy + \int_{h_1}^{H} E_2 dy \quad ; \quad K_2 = \int_0^{h_1} (E_1 \cdot y)\, dy + \int_{h_1}^{H} (E_2 \cdot y)\, dy \quad ; \quad K_3 = \int_0^{h_1} E_1 \cdot F(y)\, dy + \int_{h_1}^{H} E_2 \cdot F(y)\, dy \quad ; \\ &K_4 = \int_0^{h_1} (E_1 \cdot y^2)\, dy + \int_{h_1}^{H} (E_2 \cdot y^2)\, dy \quad ; \quad K_5 = \int_0^{h_1} E_1 \cdot y \cdot F(y)\, dy + \int_{h_1}^{H} E_2 \cdot y \cdot F(y)\, dy \quad ; \\ &K_6 = \int_0^{h_1} E_1 \cdot y^2 \cdot F(y)\, dy + \int_{h_1}^{H} E_2 \cdot y^2 \cdot F(y)\, dy \quad ; \quad K_7 = \int_0^{h_1} G_1 \cdot \left[\frac{\partial F(y)}{\partial y}\right]^2 dy + \int_{h_1}^{H} G_2 \cdot \left[\frac{\partial F(y)}{\partial y}\right]^2 dy \end{aligned} \tag{16}$$

$$\begin{aligned} &N = \int_0^{h_1} (E_1 \cdot \varepsilon)\, dy + \int_{h_1}^{H} (E_2 \cdot \varepsilon)\, dy \quad ; \quad M_1 = \int_0^{h_1} \rho_1 dy + \int_{h_1}^{H} \rho_2 dy \quad ; \quad M_2 = \int_0^{h_1} (\rho_1 \cdot y)\, dy + \int_{h_1}^{H} (\rho_2 \cdot y)\, dy \quad ; \\ &M_3 = \int_0^{h_1} \rho_1 \cdot F(y)\, dy + \int_{h_1}^{H} \rho_2 \cdot F(y)\, dy \quad ; \quad M_4 = \int_0^{h_1} (\rho_1 \cdot y^2)\, dy + \int_{h_1}^{H} (\rho_2 \cdot y^2)\, dy \quad ; \\ &M_5 = \int_0^{h_1} \rho_1 \cdot y \cdot F(y)\, dy + \int_{h_1}^{H} \rho_2 \cdot y \cdot F(y)\, dy \quad ; \quad M_6 = \int_0^{h_1} \rho_1 \cdot F(y)\, dy + \int_{h_1}^{H} \rho_2 \cdot F(y)\, dy \end{aligned} \tag{17}$$

Moreover another contribution, able to take into account the action of frictional forces at the interface between layers, can be added to Eq.14-15 . Such a model, extended to multi-layered beams with an arbitrary number of layers should be able to effectively describe the damping behaviour of composite beams constituted by layers of broadly different materials, and could be used to design coated components with specifically tailored dissipative properties.

4 Conclusions

Multiple coating solution applied to different metallic substrates were experimentally investigated. Seven tested specimens types were considered, and two coated solutions showed an improved damping behaviour with respect to uncoated ones, these solutions being a dual-layer made up of $Ti+TiO_2$ and a single-layer made up of Al oxide, both applied to an Al1000 substrate. The condensed constitutive equivalent material models of the two specimens were identified.

Further investigations need to be carried on. A wider range of coating solutions will be tested in future work to ascertain both damping behaviour and the fatigue resistance under cyclic loading. An improved multi-layered beam model, based on high order multi-layer beam theories, will be developed and experimentally validated to explore new coating solutions being optimal with respect to damping behaviour and other engineering specifications.

Acknowledgments

This study was developed within the CIRI-MAM with the contribution of the Regione Emilia Romagna, progetto POR-Fesr-Tecnopoli**.** Support from Mr.Andrea Zucchini and Marzocchi Pompe S.p.A., Casalecchio di Reno, Italy, is also kindly acknowledged.

References

[1] N.Tassini, S.Pastias, K.Lambrinou *"Ceramic coatings: A phenomenological modeling for damping behavior related to microstructural features"* Material Science and Engineering A 442 (2006) 509-513.

[2] L.Yu, Y.Ma, C.Zhou, H.Xu *"Damping efficiency of the coating structure"* International Journal of Solids and Structures 42 (2005) 3045-3058.

[3] A.I.Ustinov, B.A.Movchan *"A study of damping ability of tin-and yttrium-coated flat specimens of Ti-6%Al-4%V titanium alloy"* Strength of Materials 33(4) (2001) 339-343.

[4] J.A.Rongong, A.A.Goruppa, V.R.Buravalla, G.R.Tomlinson, F.R.Jones *"Plasma deposition of constrained layer damping coating"* Proc. Instn Mech. Engrs Vol. 218 Part C: J. Mechanical Engineering Science 218 (2004) 669-680.

[5] C.Blackwell, A.Palazzotto, T.J.George, C.J.Cross *"The evaluation of the damping characteristics of hard coating on titanium"* Shock and Vibrations 14 (2007) 37-51.

[6] F.Casadei, K.Bertoldi, D.R.Clarke *"Vibration damping of thermal barrier coatings containing ductile metallic layers"* ASME Journal of Applied Mechanics 81 (2014) 101001_1-101001_10.

[7] D.Guangyu, T.Zhen, B.Dechum, L.Kun, H.Qingkai *"Damping properties of a novel porous Mg-Al alloy coating prepared by arc ion plating"* Surface&Coatings Technology 238 (2014) 139-142.

[8] A.I.Ustinov, V.S.Skorodzievskii *"A study of the dissipative properties of homogeneus materials deposited as coatings part 2. Copper condensates with different microstructural characteristics"* Strength of Materials 40(2) (2008) 275-277.

[9] H.A.Colorado, J.Velez, H.R.Salva, A.A.Ghilarducci *"Damping behavior of physical vapor-deposited TiN coatings on AISI 304 stainless steel and adhesion determination"* Material Science and Engineering A 442 (2006) 514-418.

[10] K.A.Khor, C.T.Chia, Y.W.Gu, F.Y.C.Boey *"High temperature damping behavior of plasma sprayed NiCoCrAlY coatings"* Journal of Thermal Spray Technology 11(3) (2002) 359-364.

[11] X.Wang, Y.Pei, Y.Ma *"The effect of microstructure at interface between coating and substrate on damping capacity of coating systems"* Applied Surface Science 282 (2013) 60-66.

[12] M.Kiretseu, D.Hui, G.Tomlinson *"Advanced shock-resistant and vibration damping of nanoparticle-reinforced composite material"* Composites: Part B 39 (2008) 128-138.

[13] S.A.Reed, A.N.Palazzotto, W.P.Baker *"An experimental technique for the evaluation of strain dependent material properties of hard coatings"* Shock and Vibration 15 (2008) 697-712.

[14] S.Pastias, C.Saxton, M.Shipton *"Hard damping coatings: an experimental procedure for extraction of damping characteristics and modulus of elasticity"* Material Science and Engineering A 370 (2004) 412-416.

[15] P.J.Torvik *"Determination of mechanical properties of non-linear coatings from measurements with coated beams"* International Journal of Solids and Structures 46 (2009) 1066-1077.

[16] C.Zener *"Elasticity and anelasticity of metals"* (1948) University of Chicago Press.

[17] A.S.Nowick, B.S.Berry *"Anelastic Relaxation in Crystalline Solids"* (1972) Academic Press Inc.

[18] S.Amadori, G.Catania *"Robust identification of the mechanical properties of viscoelatic non-standard materials by means of time and frequency domain experimental measurements"* Composites Structures, Composite Structures (In Press).

[19] W.N. Finley, J.S.Lai, K.Onaran *"Creep and relaxation of nonlinear viscoelastic materials"* (1989) New York: Dover Publications Inc.

[20] L.E.S.Ramirez, C.F.M.Coimbra *"A variable order constitutive relation for viscoelasticity"* Annalen der Physik 16(7-8) (2007) 543-552.

[21] C.M.A.Vasquez, R.A.S.Moreira, R.J.Dias *"Viscoelastic damping technologies – Part 1: Modeling and finite element implementations."* Journal of Advanced Research in Mechanical Engineering 1(2) (2010) 76-95.

[22] M.H.Richardson, D.L.Formenti *"Parameter estimation from frequency response measurements using rational fraction polynomials"* (1982) 1st IMAC Conference Orlando Florida.

[23] G.E.Forsythe *"Generation and use of orthogonal polynomials for data fitting with a digital computer"* J Soc. Indust. Appl. Math. 5(2) (1957) 74-85.

[24] L.G.Kelly *"Handbook of Numerical Methods and Applications"* (1967) Addison Wesley Publishing Company.

[25] D.Liu, X.Li *"An overall view of laminate theories based on the diplacement hypothesis*" Journal of Composite Materials 30(14) (1996) 1539-1561.

[26] G.Wang, A.Unal, Q.H.Zuo *"Modelling and Analyssis of Multilayered Elastic Beam Using Spectral Finite Elwmwnt Method"* Journal of Vibrations and Acoustics 138 (2016) 041013_1-041013_12.

[27] M.Di Sciuva,M.Gherlone, L.Librescu *"Implications of damaged interfaces and of other non-calssical effevts on the load carrying capacity of multilayered composite shallow shells"* International Journal of Non-Linear Mechanics 37 (2002) 851-867.